Chemical Science

ROYAL SOCIETY OF CHEMISTRY

EDGE ARTICLE

View Article Online
View Journal | View Issue

Cite this: *Chem. Sci.*, 2021, **12**, 5926

All publication charges for this article have been paid for by the Royal Society of Chemistry

Organoruthenium-catalyzed chemical protein synthesis to elucidate the functions of epigenetic modifications on heterochromatin factors†

Naoki Kamo, [a] Tomoya Kujirai, [b] Hitoshi Kurumizaka, [b] Hiroshi Murakami, [c] Gosuke Hayashi *[c] and Akimitsu Okamoto *[ad]

The application of organometallic compounds for protein science has received attention. Recently, total chemical protein synthesis using transition metal complexes has been developed to produce various proteins bearing site-specific posttranslational modifications (PTMs). However, in general, significant amounts of metal complexes were required to achieve chemical reactions of proteins bearing a large number of nucleophilic functional groups. Moreover, syntheses of medium-size proteins (>20 kDa) were plagued by time-consuming procedures due to cumbersome purification and isolation steps, which prevented access to variously decorated proteins. Here, we report a one-pot multiple peptide ligation strategy assisted by an air-tolerant organoruthenium catalyst that showed more than 50-fold activity over previous palladium complexes, leading to rapid and quantitative deprotection on a protein with a catalytic amount (20 mol%) of the metal complex even in the presence of excess thiol moieties. Utilizing the organoruthenium catalyst, heterochromatin factors above 20 kDa, such as linker histone H1.2 and heterochromatin protein 1α (HP1α), bearing site-specific PTMs including phosphorylation, ubiquitination, citrullination, and acetylation have been synthesized. The biochemical assays using synthetic proteins revealed that the citrullination at R53 in H1.2 resulted in the reduced electrostatic interaction with DNA and the reduced binding affinity to nucleosomes. Furthermore, we identified a key phosphorylation region in HP1α to control its DNA-binding ability. The ruthenium chemistry developed here will facilitate the preparation of a variety of biologically and medically significant proteins containing PTMs and non-natural amino acids.

Received 5th February 2021
Accepted 21st March 2021

DOI: 10.1039/d1sc00731a

rsc.li/chemical-science

Introduction

Synthetic methodology for homogeneously modified proteins has been highly demanded to elucidate the biological significance of posttranslational modifications (PTMs) through biochemical and structural analysis. Total chemical protein synthesis has streamlined the preparation of target proteins bearing site-specific PTMs and functional molecules.[1–5] For example, histone proteins with various PTMs have been chemically synthesized to understand the roles of PTMs.[6] In the process of chemical protein synthesis, a target protein is divided into several peptide segments that can be synthesized by solid-phase peptide synthesis (SPPS).[7] To assemble the peptide segments, many researchers have employed native chemical ligation (NCL) that utilizes the chemoselectivity between N-terminal cysteine (Cys) and C-terminal thioester to form amide bonds between divided segments.[8] However, assembly of multiple peptide segments to obtain medium-size proteins (*e.g.*, >20 kDa) requires multiple reactions and purification steps, which causes low overall yields and time-consuming works and therefore limits the access to target proteins bearing various patterns of PTMs. To address this issue, one-pot multiple peptide ligation strategies to eliminate the intermediate purification steps, including a kinetically controlled strategy[9–11] and a protecting group-removal strategy, have been developed,[12] although these methods have been mainly exploited for the assembly of three segments to afford small proteins.

Organometallic compounds have been applied for chemical reactions on proteins, such as decaging[13,14] and bioconjugation utilizing Suzuki–Miyaura coupling,[15] Cys arylation through C–S reductive elimination using palladium (Pd) complexes,[16] or Tsuji–Trost allylations.[17,18] Recently, Brik and coworkers paved the way for the application of palladium (Pd) complexes for total

[a]*Department of Chemistry and Biotechnology, Graduate School of Engineering, The University of Tokyo, 7-3-1 Hongo, Bunkyo-ku, Tokyo 113-8656, Japan. E-mail: okamoto@chembio.t.u-tokyo.ac.jp*

[b]*Laboratory of Chromatin Structure and Function, Institute for Quantitative Biosciences, The University of Tokyo, Bunkyo-ku, Tokyo 113-0032, Japan*

[c]*Department of Biomolecular Engineering, Graduate School of Engineering, Nagoya University, Nagoya 464-8603, Japan. E-mail: hayashi@chembio.nagoya-u.ac.jp*

[d]*Research Center for Advanced Science and Technology, The University of Tokyo, Meguro-ku, Tokyo 153-8904, Japan*

† Electronic supplementary information (ESI) available. See DOI: 10.1039/d1sc00731a

chemical protein synthesis.[19–28] They exploited several protecting groups that were labile by specific Pd complexes for chemoselective masking and one-pot ligation of peptide segments.[21,24] Our group employed allyloxycarbonyl (alloc) groups for the protection of N-terminal Cys, which were removed with Pd/3,3′,3″-phosphanetriyltris(benzenesulfonic acid) trisodium salt (TPPTS) complexes.[29] The one-pot peptide ligation using Pd/TPPTS complex allowed us to synthesize histone H2AX efficiently. However, the repetitive metal-mediated decaging reactions to ligate multiple peptide segments necessitated considerable amounts of metal complexes especially under NCL conditions containing an excess amount of thiol compounds that significantly degrade metal complexes.[29] Generally, decaging or cross-coupling reactions on protein surfaces under aqueous conditions require excessive amounts of metal complexes[13,14] probably because nucleophilic functional groups on proteins such as thiol groups[30] would readily coordinate to metal complexes. Moreover, some metal complexes (*e.g.*, Pd/TPPTS complexes) are very unstable under aerobic conditions, and these organometallic compounds required strict deoxygenated conditions. Furthermore, a high loading of transition metal complexes often cause protein aggregations,[31] which interferes with the whole synthetic procedure to obtain target proteins. To overcome these problems, a highly active organometallic compound that minimizes the metal loading has been demanded in chemical protein synthesis to produce a variety of proteins of interest with modifications and accelerate biological research.

In this study, we focused on organoruthenium complexes to achieve decaging reactions on polypeptides in catalytic manners. After our screening of metal complexes, we discovered air-tolerant ruthenium (Ru) complexes that showed more than 50-fold catalytic activity compared with previous Pd complexes for the decaging reaction and only 20 mol% of an organoruthenium catalyst allowed the deprotection of the alloc groups on polypeptides under NCL conditions. The new one-pot multiple peptide ligation strategy, including consecutive more than five reaction steps using the Ru catalyst, was applied for the total chemical synthesis of linker histone H1.2 (size: 22 kDa) and heterochromatin protein 1α (HP1α) (size: 22 kDa). Our new streamlined synthetic method afforded homogeneous two kinds of H1.2s and six kinds of HP1α bearing different patterns of PTMs including phosphorylation, ubiquitination, citrullination, and acetylation. Finally, we investigated the effects of those PTMs decorated in heterochromatin factors on chromatosome formations or the binding ability toward DNA to elucidate the functions of the epigenetic marks.

Results and discussion

Exploration of organoruthenium complexes

Under NCL conditions involving excess MPAA, the metal complexes lost activity rapidly because of its sulfur poisoning effect. Therefore, it was important to increase the stability of the metal complexes under NCL conditions to achieve catalytic reactions on peptides or proteins. To accomplish this goal, we focused on Ru complexes rather than Pd complexes. Electron-rich Pd (10 outer electrons) forms a strong bond with thiol moieties because of the π-back donation from Pd to the empty relatively low-energy d orbitals of the sulfur.[32] On the other hand, electron-deficient Ru (8 outer electrons) favors ionic interactions to fill its d orbital and does not form a strong coordination bond with soft nucleophiles.[33] Moreover, electron-rich Pd is more sensitive to electronic modification by sulfur poisoning, which causes significant changes in catalytic activity, than electron-poor Ru.[33] When we screened trivalent phosphine ligands for Pd, we could not discover more active ligands for the alloc removal than TPPTS (Fig. S1†). Although the Pd loading on proteins could be reduced by the addition of magnesium ion,[21,34] these results suggested that it would be difficult to deprotect the alloc groups on peptides under NCL conditions with Pd complexes in catalytic manners. Meanwhile, some researchers reported that organoruthenium complexes tolerated sulfur poisoning and catalyzed the allyl transfer to thiol moieties,[35] but these Ru complexes had not been applied for chemical reactions on biomolecules. To test whether organoruthenium complexes could sustain the catalytic activity for the removal of the alloc group on a peptide under NCL conditions and air atmosphere, we prepared Cp*Ru(cod)Cl (**Ru-1:** Cp* = η^5-pentamethylcyclopentadienyl, cod = η^4-1,5-cyclooctadiene), [Cp*Ru(QA)allyl]PF_6 (**Ru-2:** QA = 2-quinolinecarboxylate), [CpRu(QA)allyl]PF_6 (**Ru-3:** Cp = η^5-cyclopentadienyl), [CpRu(QA-NMe_2)allyl]PF_6 (**Ru-4:** QA-NMe_2 = 4-(*N*,*N*-dimethylamino)-2-quinolinecarboxylate) bearing *N*,*O*-bidentate ligand (Table 1).[36–38] Next, we tested the alloc deprotection on peptide **1** with 10 mol% of metal complexes under NCL conditions (Table 1), and the conversion yields were calculated based on high-performance liquid chromatography (HPLC). In previous research, 2 equiv. of Pd/TPPTS complex was required to attain quantitative removal of the alloc groups under NCL conditions.[29] When the amount of the Pd complex was reduced to 10 mol%, the conversion yield reached to only 12% after 3 h (Table 1, entry 1), indicating that the TON of Pd/TPPTS complexes under NCL conditions was 1.2. In contrast, **Ru-1** and **Ru-2** sustained the catalytic activity even in the presence of a high concentration of MPAA (entries 2 and 3) under air atmosphere, and quantitative removal of the alloc groups was observed after 2 h upon the treatment with 10 mol% **Ru-2** (entry 3). Furthermore, only 5 mol% of **Ru-3** or **Ru-4** rapidly catalyzed the alloc deprotection, and the reaction reached completion within 10 min (entries 6 and 7). We did not observe any side reactions, such as the transfer of the allyl groups to nucleophilic functional groups at side chains of peptide **1** (Fig. S2†). The slow reaction rate of **Ru-2** compared to **Ru-3** could be explained by the sterically hindered Cp* disturbing nucleophilic attack of MPAA toward π-allyl Ru complex, which was already reported.[38] We should note that the activity of the Ru catalysts diminished in the presence of TCEP (entries 8–11); however, oxidized TCEP after the reduction of the disulfide bond of MPAA dimer did not affect the activity of **Ru-4** (entry 12, Fig. S3†). We screened other Ru complexes for the alloc deprotection under NCL conditions. We replaced the *N*,*O*-ligand with an *N*,*N*-ligand, and synthesized [Cp(η^2-bipy)(η^3-allyl)Ru^{IV}][PF_6]$_2$ (**Ru-5:** bipy = bipyridine) and [Cp(η^2-phen-NMe_2)(η^3-allyl)Ru^{IV}][PF_6]$_2$ (**Ru-6:** phen = phenanthroline).[39] However, the catalytic activities of **Ru-5** and **Ru-6** were much lower than those of

Table 1 Deprotection of the alloc group of peptide **1** with Pd or Ru complexes under NCL conditions

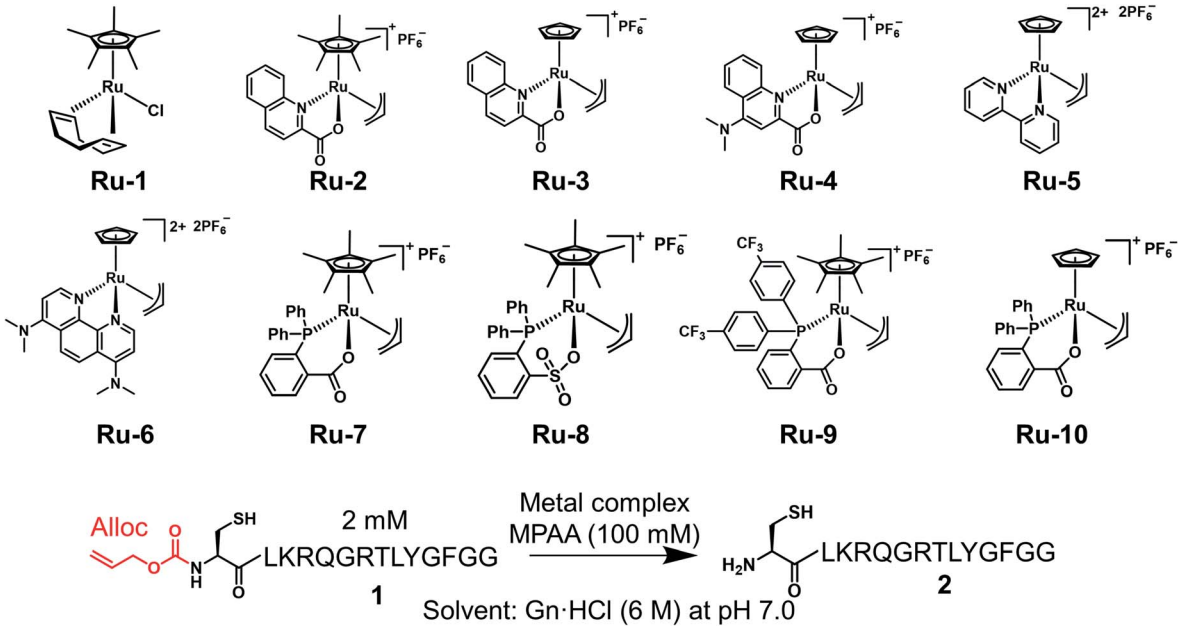

				Conversion yields[a] [%]				
Entry	Metal complexes	Quantity (mol%)	Additive	10 min	30 min	1 h	2 h	3 h
1	Pd/TPPTS	10	—	11	11	12	12	12
2	**Ru-1**	10	—	28	56	76	86	94
3	**Ru-2**	10	—	41	76	92	>95	—
4	**Ru-3**	10	—	>95	—	—	—	—
5	**Ru-4**	10	—	>95	—	—	—	—
6	**Ru-3**	5	—	>95	—	—	—	—
7	**Ru-4**	5	—	>95	—	—	—	—
8	**Ru-3**	5	TCEP (3 mM)	65	67	67	70	72
9	**Ru-3**	5	TCEP (10 mM)	<5	<5	7	—	—
10	**Ru-4**	5	TCEP (3 mM)	55	67	69	75	78
11	**Ru-4**	5	TCEP (10 mM)	8	9	10	—	—
12	**Ru-4**	5	TCEP (5 mM)[b]	>95	—	—	—	—
13	**Ru-5**	5	—	<5	<5	<5	<5	6
14	**Ru-6**	5	—	7	10	14	17	17
15	**Ru-7**	5	—	19	40	60	76	80
16	**Ru-8**	5	—	<5	18	47	64	71
17	**Ru-9**	5	—	18	36	53	73	76
18	**Ru-10**	5	—	93	>95	—	—	—
19	**Ru-10**	5	TCEP (3 mM)	50	61	66	68	68
20	**Ru-10**	5	TCEP (10 mM)	<5	<5	11	—	—

[a] The conversion yields were calculated from peak areas analyzed by HPLC (Fig. S2). [b] TCEP was completely consumed for the reduction of MPAA disulfide dimer before the addition of **Ru-4** as shown in Fig. S3.

Ru-3 or **Ru-4** (entries 13 and 14) probably because of those rigid structures.

Previous research showed that the rate-determining step of the alloc removal using **Ru-3** or **Ru-4** was the oxidative addition of the allyl groups toward Ru when strong nucleophiles, such as thiol moieties, were employed.[38] To accelerate the uncaging of the alloc groups and further improve the stability under NCL conditions, we focused on *P*,*O*-bidentate ligands to replace *N*,*O*-ligands, and increase the electron density of Ru complexes. Bruneau and coworkers reported Ru complexes coordinated by *o*-diphenylphosphino benzoate (*o*-DPPBz) or diphenylphosphinobenzene sulfonate (*o*-DPPBS).[40] We synthesized [Cp*Ru(κ^2-*o*-DPPBz)allyl]PF_6 (**Ru-7**) and [Cp*Ru(κ^2-*o*-DPPBS)allyl]PF_6 (**Ru-8**) (Table 1) and tested those catalytic activities. There was no significant difference between **Ru-7** and **Ru-8** (entries 15 and 16) for the alloc deprotection of peptide **1** under NCL conditions. To reduce the electron density of the phosphine ligand and enhance the nucleophilic attack of MPAA toward π-allyl Ru

complexes, we synthesized Ru complexes coordinated by *o*-DPPBz bearing CF_3 groups (**Ru-9**), but no improvement of these Ru complexes over **Ru-7** was observed (entry 17). Considering the effective deprotection of the alloc group using **Ru-3** compared to **Ru-2** (entries 3 and 4), we newly synthesized [CpRu(κ^2-*o*-DPPBz)allyl]PF_6 (**Ru-10**). The deprotection efficiency was dramatically improved by replacing Cp* with Cp, and the reaction reached completion within 30 min (entry 18), although the catalytic activity of **Ru-10** was also reduced in the presence of TCEP (entries 19 and 20). We concluded that organoruthenium catalysts coordinated by Cp and *X*,*O*-bidentate ($X = N$ or P) ligand efficiently catalyzed the removal of the alloc group under NCL conditions.

Calculation of TON of Ru catalysts

We examined TON and turnover frequency (TOF) of **Ru-3**, **Ru-4**, and **Ru-10**, which removed the alloc groups quantitatively with 5 mol% catalysts. We reduced the amount of each Ru complex to 1 mol% and tested the removal of the alloc group of peptide **1** under NCL conditions (Fig. 1). **Ru-3** (TOF: 19 min^{-1}) and **Ru-4** (TOF: 20 min^{-1}) showed similar TOF value, but the TON of **Ru-4** (TON: 70) was slightly higher compared to **Ru-3** (TON: 56), because of the NMe_2 group in **Ru-4**, which increased the electron density of Ru and its stability against excess MPAA. The reaction rate using **Ru-10** (TOF: 6 min^{-1}) as a catalyst was slower than **Ru-3** or **Ru-4** due to the steric hindrance of the *P*,*O*-bidentate ligand of **Ru-10**, but **Ru-10** sustained its catalytic activity for a longer time because of its stability and showed similar catalytic activity (TON: 72) to that of **Ru-4** and higher than that of **Ru-3**. We further calculated the electrophilicity of each Ru catalyst based on density functional theory (DFT). The lowest unoccupied molecular orbital (LUMO) level of *o*-DPPBz was more than 0.5 eV higher than QA and QA-NMe_2 (−1.44 eV *vs.* −2.15 eV *vs.* −1.94 eV) (Fig. S5†). This higher π-accepting ability of QA or QA-NMe_2 led to the higher electrophilicity of **Ru-3** or **Ru-4** and the attack of MPAA toward π-allyl Ru complexes became faster than **Ru-10**. To summarize, compared to the activity of Pd/TPPTS complexes (TON: 1.2), **Ru-4** and **Ru-10** showed more than 50-fold catalytic activity, and catalytically removed the alloc groups of peptides under aqueous conditions and even in the presence of 5000 equiv. of MPAA that normally poisoned organometallic catalysts.

To further explore the difference between **Ru-4** and **Ru-10**, we added these Ru complexes to a solution containing peptide **1** without MPAA, a scavenger for π-allyl Ru complexes (Fig. S6†). When 10 mol% of **Ru-4** was tested, peptide **1** was completely consumed within 30 min, and single or double allyl transfer to functional groups of peptides was observed. Based on MS/MS analysis of each HPLC peak (Fig. S7†), it was found that the allyl groups were transferred to amine groups or thiol groups of N-terminal Cys, not to other amino acids, such as Lys, Tyr, or Thr. When 10 mol% of **Ru-10** was examined, the starting material remained for over 1 h reaction, and the allyl transfer to peptide **1** barely occurred (Fig. S6†). These results indicated that **Ru-4** was more reactive with nucleophiles than **Ru-10** because of its more electrophilic π-allyl Ru complex, which presented the possibility of side reactions, such as allyl transfer to the functional groups of peptides *via* **Ru-4**. However, in the presence of excess MPAA (pK_a 6.6),[41] this strong nucleophile attacked π-allyl Ru complex before peptides and suppressed the undesired reactions as observed by comparing HPLC data shown in Fig. S2 and S6.†

Inactivation by MPAA to form a binuclear Ru complex

To achieve one-pot peptide ligation by repeating the cycles of NCL and decaging, the deactivation of metal complexes just before the subsequent NCL was a critical step.[29] Therefore, we investigated the deactivation of **Ru-4** or **Ru-10** under NCL conditions (Fig. S8†). 200 mol% of Pd/TPPTS complex against peptide **1** was rapidly deactivated by 100 mM MPAA and lost activity within 10 min

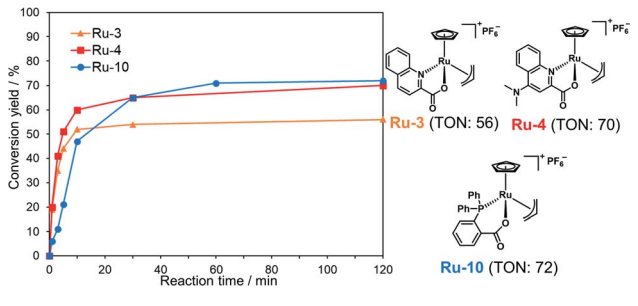

Fig. 1 Calculation of TON and TOF of 1 mol% **Ru-3**, **Ru-4**, or **Ru-10** for the deprotection of the alloc group of peptide **1** (2 mM) in NCL buffer [Gn·HCl (6 M), NaH_2PO_4 (200 mM), MPAA (100 mM, 5000 equiv. against the Ru catalyst) at pH 7.0]. The conversion yields under different conditions are shown in Table S1.†

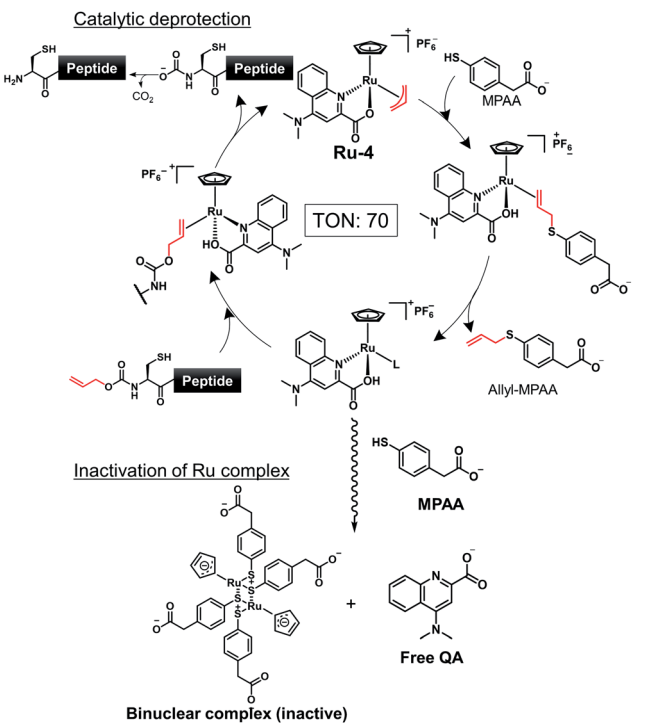

Scheme 1 Simultaneous catalytic alloc deprotection and deactivation of **Ru-4**.

(Table S2,† entry 1). In contrast, 10 mol% of **Ru-4** and **Ru-10** against peptide **1** showed stability under NCL conditions (entries 2 and 3), and **Ru-10** was more stable than **Ru-4** because of its bulky *P*,*O*-bidentate ligand. We concluded that the greater stability of these Ru complexes over Pd complexes contributed to the catalytic activity for the removal of the alloc groups of peptides. By NMR and MALDI-TOF mass analysis, the half-sandwich Ru complex reacted with MPAA to form a binuclear Ru complex,[42] which might be inactive for the alloc removal (Fig. S9 and S10†). Moreover, we observed the detachment of the bidentate ligand from Ru through the ligand exchange with MPAA.

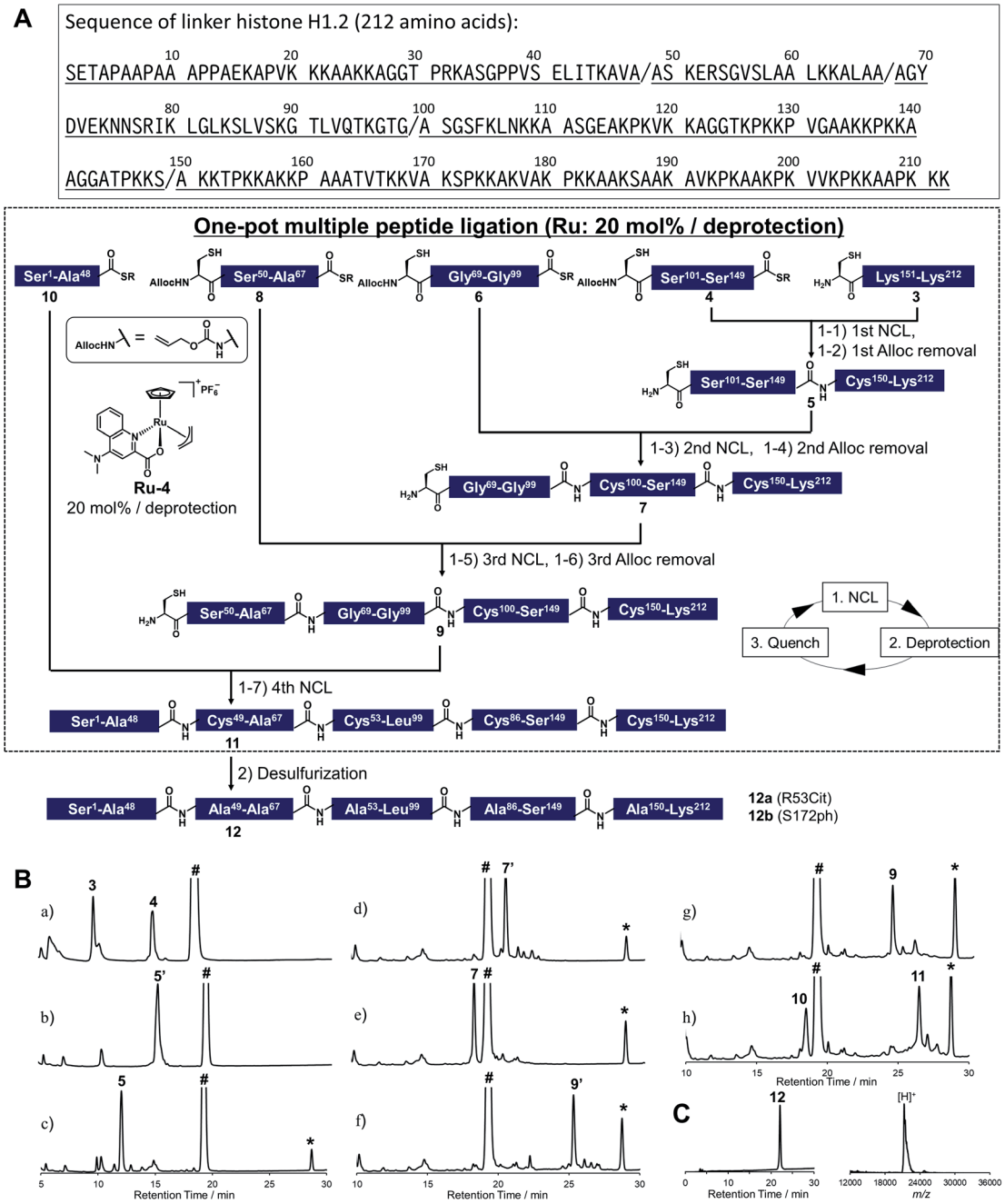

Fig. 2 Chemical synthesis of linker histone H1.2 using the Ru catalyst. (A) Synthetic strategy. / represents the cleavage sites. (1) NCL condition: peptides (2 mM), MPAA (100 mM) in denaturing buffer at pH 7.0, 37 °C. Removal condition: **Ru-4** (20 mol%), 37 °C, 30 min. (2) Peptide (0.8 mM), TCEP (300 mM), GSH (150 mM), VA-044 (20 mM) in denaturing buffer at pH 7.0, 37 °C. (B) Reaction tracking of the one-pot ligation involving catalytic amount of **Ru-4** (20 mol%) for the alloc deprotection by analytical HPLC (gradient: 10–46% for 30 min) at 220 nm. Compounds **5′**, **7′**, and **9′** are the alloc-protected peptides **5**, **7**, and **9**, respectively. # = MPAA. * = allyl-transferred MPAA. (a) 1st NCL (t = 2 min). (b) 1st NCL (t = 2 h). (c) 1st deprotection. (d) 2nd NCL (t = 2 h). (e) 2nd deprotection. (f) 3rd NCL (t = 2 h). (g) 3rd deprotection. (h) 4th NCL (t = 2 h). (C) HPLC profile (left, gradient 20–50% for 30 min) and MALDI-TOF mass spectrum (right) of purified peptide **12**. Calculated mass of **12** $[M + H]^+$: 21 276.6; mass found $[M + H]^+$: 21 277.8.

To summarize, the alloc deprotection of peptides based on the Tsuji–Trost reaction mechanism catalyzed by the Ru catalysts under NCL conditions proceeded very fast, and the reaction reached completion within 10 min. Along with the deprotection, the Ru catalyst slowly lost the catalytic activity through ligand exchange with MPAA to form a binuclear complex, enabling the subsequent NCL with alloc-protected peptides (Scheme 1). Newly synthesized **Ru-10** coordinated by *P*,*O*-ligands showed the highest catalytic activity and the greatest stability under NCL conditions among tested Ru complexes. However, considering the facile deactivation by MPAA, we decided to employ **Ru-4** to attain total chemical synthesis of proteins through one-pot multiple peptide ligation.

Chemical synthesis of histone H1.2 assisted by an organoruthenium catalyst

To demonstrate the utility of **Ru-4** catalyst for chemical protein synthesis, we selected linker histone H1.2 as a target protein. This protein interacts with nucleosomes to form chromatosomes and contributes to the formation of a higher-order chromatin structure.[43–46] Previous papers reported that various PTMs can be decorated on H1.2, and some of these modifications play roles in chromatin decondensation.[47] However, it had been challenging to achieve the chemical synthesis of H1.2 compared to core histone proteins (<140 amino acids), because of its large size (212 amino acids). Therefore, we aimed to establish a synthetic method to obtain H1.2 through one-pot multiple peptide ligation using **Ru-4**.[48]

As shown in Fig. 2A, Cys mutations for NCL reactions were incorporated at Ala sites ($A^{48}C$, $A^{68}C$, $A^{100}C$, $A^{150}C$) and divided into five peptide segments of H1.2 (peptides **3**, **4**, **6**, **8**, and **10**), which were synthesized by 9-fluorenylmethyloxycarbonyl SPPS (Fmoc-SPPS) (Fig. S11†). The N-terminal Cys of peptides **4**, **6**, and **8** were protected by the alloc groups, and the one-pot five-segment ligation using **Ru-4** was performed. All the NCL reactions and the removal of alloc groups were conducted in NCL buffer (6.0 M guanidinium chloride, 200 mM NaH_2PO_4, 100 mM MPAA) at 37 °C.

Peptides **3** and **4** (1.1 equiv. relative to peptide **3**) were dissolved in NCL buffer, and the NCL reaction reached completion within 2 h to afford peptide **5** (Fig. 2B). **Ru-4** (0.2 equiv.) was added to the reaction solution, and the mixture was stirred for 30 min to remove the alloc group and fully deactivate **Ru-4**. After completion, a small amount of TCEP solution was added to reduce disulfide bonds and be consumed completely to minimize the effect on the next alloc removal with **Ru-4** (Fig. S3†). Powdered peptide **6** was then added to initiate the second NCL reaction. These operations were repeated for the second deprotection and the third NCL and deprotection (Fig. 2B).

Finally, powdered peptide **10** was added to initiate the fourth NCL reaction. HPLC analysis showed a major peak corresponding to the desired ligated peptide **11** (Fig. 2B) after seven consecutive reaction steps. The reaction product was purified by HPLC, and 2.52 mg of peptide **11** was obtained in 23% yield from **3** (Fig. S13†). Compared to the previous one-pot ligation method with Pd/TPPTS complex,[29] the total amount of metal complexes was reduced to 0.6 equiv. (Pd: more than 6.0 equiv.), and strict deoxygenated conditions established by argon bubbling were not required during the procedure. The mutated Cys residues were converted into original Ala residues by free-radical desulfurization[49] to afford 1.34 mg of full-length H1.2 (**12**) almost quantitatively (Fig. 2C). Analysis by inductively coupled plasma mass spectrometry (ICP-MS) showed that the quantity of Ru attached to synthesized H1.2 was only 0.000037% (w/w) (Table S3†), and the amount of metal was much lower compared to the Pd content on previously synthesized histone H2AX (0.00096%) produced by one-pot ligation using Pd/TPPTS complexes.[29]

Next, we decided to incorporate PTMs into H1.2. As candidates of modifications, we chose citrullination of 53rd Arg (R53Cit) and phosphorylation of 172nd Ser (S172ph). It was reported that the R53 site was modified to Cit by peptidyl arginine deiminase 4 (PAD4), which regulates pluripotency, and the chromatin structure became decondensed and cells were reprogrammed.[50] S172ph was observed specifically during interphase and mitosis and might have an influence on the stability of chromatosome.[51] Therefore, we tried to investigate the effects of these PTMs on the binding affinity of H1.2 for nucleosome by creating homogeneously modified proteins. To synthesize modified H1.2, we prepared a peptide segment of H1.2 bearing R53Cit (**8a**) or S172ph (**3a**) by Fmoc-SPPS (Fig. S10†). According to Fig. 2A, the divided peptide segments were assembled in a one-pot manner with the Ru catalyst (Fig. S13†). After completion of all peptide ligations and purification, the Cys residues were converted into Ala residues. As a result, we accomplished the chemical synthesis of citrullinated H1.2 (**12a**) and phosphorylated H1.2 (**12b**) at mg scale (Fig. S14†). Thus, our facile and rapid synthetic method helped the efficient chemical synthesis of three types of full-length H1.2.

Reconstitution of chromatosomes

We examined the formation of chromatosomes using our synthetic H1.2 (Fig. 3A). The recombinant H1.2 or synthetic H1.2 (**12**) was mixed with Nap1, a histone chaperone to suppress aggregation during the reconstitution of chromatosomes,[52] and each mixture was incubated at 37 °C. The nucleosome solution was then added to each mixture to reconstitute chromatosomes. The synthetic H1.2 (**12**) formed chromatosomes in a similar way to recombinant H1.2 (Fig. S16†), suggesting that synthetic H1.2 was refolded properly for chromatosomes formations.

Next, we investigated the effect of R53Cit or S172ph on the binding affinity for nucleosome by electrophoretic mobility shift assay (EMSA) (Fig. 3B). There was a slight difference between **12** and **12b** with phosphorylation, but **12a** with citrullination reduced its binding affinity for nucleosomes, and its conversion yield was reduced by approximately 30% compared to nonmodified H1.2 (Fig. 3C). R53 interacts with the phosphate backbone of the minor groove of linker DNA in chromatosome (Fig. 3D).[53]

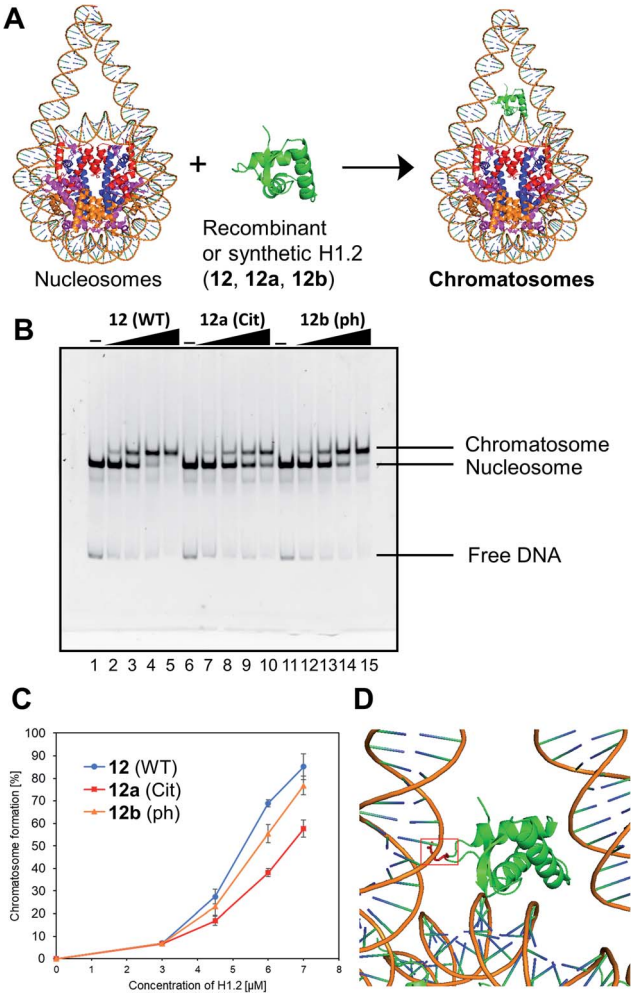

Fig. 3 Gel band shift assay for reconstitution of chromatosomes. (A) Schematic representation of the reconstitution of chromatosomes. (B) Representative gel image of the H1.2 binding assay. Increasing amounts of wt H1.2, H1.2 bearing R53Cit, or H1.2 bearing S172ph (0 μM: lanes 1, 6 and 11; 0.3 μM: lanes 2, 7 and 12; 0.45 μM: lanes 3, 8 and 13; 0.6 μM: lanes 4, 9 and 14; 0.7 μM: lanes 5, 10 and 15) were mixed with nucleosomes (0.1 μM) in the presence of Nap1 (0.3 μM). After incubation at 37 °C, the complexes were detected by nondenaturing 5% PAGE with ethidium bromide staining. (C) Quantification of EMSAs using synthetic H1.2s. (D) Position of R42 (red) of *X. laevis* histone H1.0b, which is identical to R53 of human H1.2, in chromatosomes (PDB: 5NL0).[53]

We concluded that H1.2 with R53Cit reduced its binding ability toward nucleosomes because of the lack of electrostatic interaction between Arg and DNA, which would contribute to the relaxation of chromatin and reprogramming of cells.[50] By our research using homogeneously modified H1.2, the direct effects of PTMs of H1.2 were examined.

Chemical synthesis of HP1α with Ru-4

To broaden the applicability of the organoruthenium-catalyzed chemical protein synthesis, we selected heterochromatin protein 1α (HP1α) as a second target. This protein contains two globular domains, a chromo domain (CD) and a chromo shadow domain (CSD), which are connected by a hinge region (HR).[54–57] CD recognizes the trimethylation of Lys 9 within histone H3 (H3K9me3), a hallmark of transcriptionally silenced chromatin.[58] CSD is a domain responsible for the self-dimerization of HP1α, and also provides the interface to interact with proteins bearing the PXVXL/I binding motif, such as shugoshin 1 (Sgo1).[59] In the presence of H3K9me3, CD interacts with this modification and CSD forms intermolecular bridging, which condenses chromatin to form transcriptionally silenced states.[60] HP1α was reported to be extensively decorated with PTMs,[61] and these PTMs affected the interaction pattern, distribution, and localization of HP1α.[57] Therefore, the elucidation of the functions of PTMs on HP1α was essential to understand the behaviour of dynamic chromatin.

In accordance with Fig. 4A, Cys mutations for NCL reactions were incorporated at Ala sites ($A^{98}C$, $A^{129}C$, $A^{153}C$), and full-length HP1α was divided into five peptide segments (peptides **13**, **14**, **15**, **16**, **20**), and each segment was synthesized by Fmoc-SPPS (Fig. S17†). C-terminal Asp 58, bearing thioesters of peptide **20**, was protected by the allyl group to inhibit hydrolysis of thioesters and isomer formation *via* intramolecular cyclization.[62,63] The N-terminal Cys of peptides **14** and **15** were protected with the alloc groups, and acetamidomethyl (acm) groups were introduced at N-terminal Cys of peptide **16** (C^{59}) and inner Cys of peptides **13** (C^{160}). Furthermore, to improve the solubility of peptide **14**, we installed a solubilizing tag bearing phenylacetamidomethyl (phacm) group at C^{133} site, which was removed in the same deprotection method as acm groups.[22]

Peptides **13**, **14**, **15**, and **16** were assembled in a one-pot manner using **Ru-4** catalyst (Fig. 4B). The removal of the alloc groups proceeded with only 20 mol% of **Ru-4**, and, after three NCL steps and two deprotection steps, the desired intermediate peptide **17** was obtained in 35% isolated yield (Fig. S18 and S19†). Free-radical desulfurization was then performed to convert mutated Cys residues into original Ala residues (Fig. S20†). To remove the acm groups and solubilizing tag, we first employed sodium tetrachloropalladate (Na_2PdCl_4).[21,64] As a result, after the addition of this Pd complex (5.0 equiv. toward peptide **18**), some aggregates appeared in the reaction solution, which led to low recovery rates after HPLC purification (Fig. S21†). Therefore, we used silver acetate (AgOAc) instead of Na_2PdCl_4.[65] This time, aggregates were not observed after the overnight reaction and the desired product **19** was isolated in 62% yield (Fig. S22†). Finally, peptide **20** was ligated with peptide **19**, and the reaction reached completion after 2 h (Fig. 4C). When we successively added Pd/TPPTS complex to remove the ally group at Asp 58, some aggregates appeared again. When we analyzed the aggregation of full-length HP1α in the presence of Pd or Ru by dynamic light scattering (DLS), the catalytic amount of Ru did not contribute to the formation of the aggregates (Fig. S24†). Therefore, **Ru-4** was used for deprotection of the allyl group, and the desired full-length HP1α (**21**) was obtained without aggregation in 53% isolated yield (Fig. 4D). The measurement of Ru content by ICP-MS showed that 0.00011% of Ru was attached on **21** (Table S3†). The circular dichroism spectrum of **21** was measured after refolding (Fig. 4E), and the ellipticity around 208–218 nm of **21** was lower than that of recombinant HP1α, indicating that the antiparallel

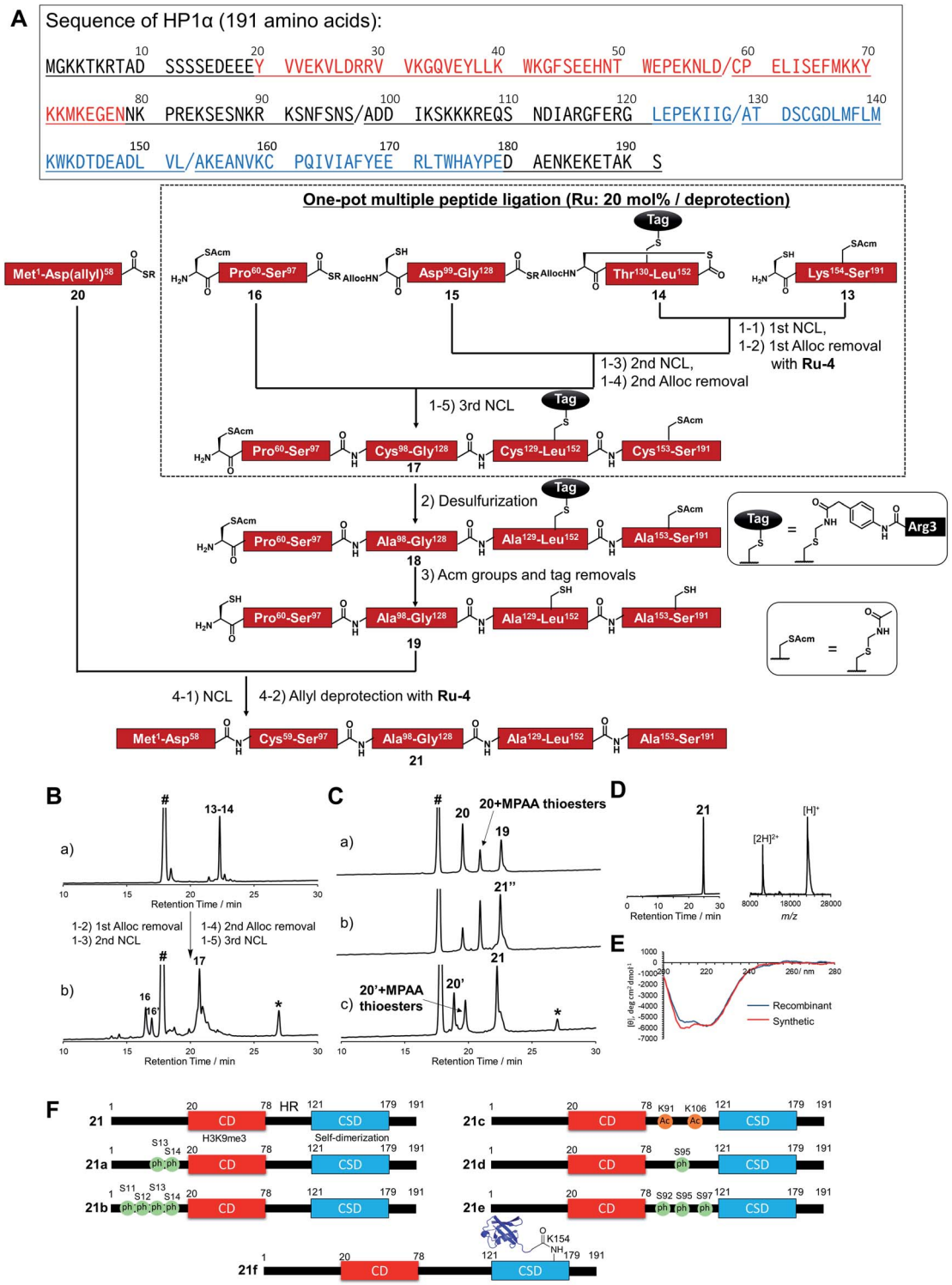

Fig. 4 Chemical synthesis of HP1α using the Ru catalyst. (A) Synthetic strategy. / represents the cleavage cites. Red region represents chromodomain, underlined region represents hinge region, and blue region represents chromo shadow domain of HP1α. (1) NCL condition: peptides (2 mM), MPAA (100 mM) in denaturing buffer at pH 7.0, 37 °C. Removal condition: **Ru-4** (20 mol%), 37 °C, 30 min. (2) Peptide (0.8 mM), TCEP (300 mM), GSH (150 mM), VA-044 (20 mM) in denaturing buffer at pH 7.0, 37 °C, overnight. (3) Peptide (0.5 mM), AgOAc (30 mM), H_2O/AcOH (1 : 1), 37 °C, overnight. (4) NCL condition: peptides (1.5 mM), MPAA (100 mM) in denaturing buffer at pH 7.0, 37 °C. Removal condition: **Ru-4** (20 mol%), 37 °C, 30 min. (B) Reaction tracking of the one-pot ligation with a catalytic amount of **Ru-4** (20 mol%) for the alloc deprotection by analytical HPLC (gradient: 15–51% for 30 min) at 220 nm. (a) 1st NCL (t = 4 h). (b) 3rd NCL after overnight reaction. (C) Reaction tracking of NCL between peptides **19** and **20**, followed by the allyl removal with **Ru-4** (20 mol%) by analytical HPLC (gradient: 15–51% for 30 min) at 220 nm. (a) NCL (t = 3 min). (b) NCL (t = 1.5 h). (c) Allyl deprotection with **Ru-4**. **21″** = **21** bearing allyl-protected Asp 58. (D) HPLC profile (gradient 15–51% for 30 min) and MALDI-TOF mass spectrum of purified peptide **21**. Calculated mass of **21** $[M + H]^+$: 22 225.7; mass found $[M + H]^+$: 22 226.0. (E) CD spectrum of **21**. (F) Chemically synthesized HP1α with PTMs in this study. **21**: HP1α without PTMs. **21a** and **21b**: HP1α with PTMs at N-terminus. **21c**, **21d**, and **21e**: HP1α with PTMs at HR. **21f**: HP1α with Ub at K154 at CSD.

β sheet of **21** was more stabilized compared to commercially available recombinant HP1α. To summarize the chemical synthesis of HP1α, it would be difficult to apply Pd complexes for HP1α due to the aggregation probably caused by intermolecular bridging of Cys of HP1α by Pd complexes and hydrophobic interactions among CSDs. These results emphasized that the choice of an adequate metal complex was crucial to produce a target protein.

Preparation of a diversity of HP1α with different patterns of PTMs

We then tried to create HP1α bearing specific PTMs. First, we focused on phosphorylations decorated at Ser residues of the N-terminal tail of HP1α (S11, S12, S13, S14),[66] which increase its binding affinity toward H3K9me3 and disturb the interaction between DNA and basic patches in HR of HP1α (residues 89–91 and residues 104–107).[67] However, the effect of the number of phosphorylated Ser at the N-terminal tail had not been investigated. Moreover, it was reported that Ser residues of HR in mouse HP1α are phosphorylated in cells.[66,68] S95ph mediated by NDR1 kinase is required for mitotic progression and Sgo1 binding to mitotic centromeres,[69] and Aurora B kinase also mediates mitotic phosphorylation of HP1α at HR (mainly at S92).[70] To investigate the effect of the phosphorylation at HR on the DNA binding affinity of HP1α, phosphorylated HP1α was prepared by enzymatic methods.[66,70] However, the possibility of phosphorylations at other Ser sites by kinases could not be excluded and homogeneous HP1α bearing site-specific phosphorylations were required to investigate the precise property of each phosphorylation site. On the other hand, although the responsible enzymes had not been discovered, Lys 91 and Lys 106 in basic areas of HP1α were reported as decorated with acetylation,[61] but the influence of acetylation on DNA binding was still unclear. To construct homogeneously phosphorylated or acetylated HP1α, we newly synthesized peptides **15a**, **16a**, **16b**, **16c**, **20a**, and **20b** by Fmoc-SPPS (Fig. S17†). By following the synthetic scheme shown in Fig. 4A, we constructed double phosphorylated (S13ph, S14ph) (**21a**) and quadruple phosphorylated (S11ph, S12ph, S13ph, S14ph) (**21b**) HP1α at the N-terminus, singly phosphorylated (S95ph) (**21c**) and triple phosphorylated (S92ph, S95ph, S97ph) (**21d**) HP1α at HR and double acetylated (K91ac, K106ac) (**21e**) HP1α at HR (Fig. 4F).

We also focused on the PTMs decorated at CSD of HP1α. Ubiquitination (Ub) at K154 promotes the degradation of HP1α through the autophagy pathway to enable efficient DNA repair.[71] K154 is located at the dimerization interface of CSDs, and we hypothesized that steric hindrance of Ub might disturb the dimerization of CSD and interaction with proteins bearing the PXVXL/I binding motif to relax chromatin structures. To create HP1α with Ub at K154, we synthesized peptides **22** and **23** (Fig. S26†). Peptide **22**, which contained the C-terminal region of Ub linked by isopeptide linkage at K154 of HP1α, was prepared in a similar way to previous research (Scheme S2†).[72] To achieve one-pot synthesis by combining the convergent method, peptide **24**, bearing acyl hydrazide at its C-terminus, was also synthesized. Peptides **14**, **22**, **23**, and **16–24** were assembled in a one-pot manner using **Ru-4** to obtain peptide **25** (Fig. S27 and S28†), and, after desulfurization followed by the removal of the acm groups and the solubilizing tag (Fig. S29 and S30†), peptide **27** was ligated with peptide **20** followed by the allyl deprotection with **Ru-4** to afford HP1α ubiquitinated at K154 (**21f**) (>30 kDa) (Fig. 4F and S31†). Finally, we obtained six kinds of full-length HP1α bearing the different patterns of PTMs. We note that these proteins were rapidly prepared owing to one-pot ligation of divided peptide segments using only catalytic amounts of organoruthenium complexes.

Fluorescence anisotropy assay of synthesized HP1α

After refolding of chemically synthesized HP1α by dialysis, we first tested the interaction of the CD of HP1α with H3K9me3 peptide bearing fluorescein at its N-terminus (residues 1–20) by fluorescence anisotropy assay. The binding affinity of **21** [dissociation constant (K_d): 23 μM] was almost the same as that of recombinant HP1α (K_d: 19 μM) (Fig. 5A and S32†), indicating that the CD of synthetic HP1α properly recognized the H3K9me3 mark. We further examined the binding of Sgo1 peptide (residues 446–466) bearing fluorescein toward dimerized interfaces of HP1α CSDs. **21** showed a similar K_d value (K_d: 0.47 μM) toward Sgo1 peptide as the recombinant one (K_d: 0.51 μM). These results indicated that our chemically synthesized HP1α was properly refolded, and recognized H3K9me3 modification and PXVXL/I binding motif through CD and dimerized CSDs, respectively. Next, we investigated the influence of Ub at K154 of HP1α on the binding ability toward the Sgo1 peptide. The K_d value of **21f** was increased to 1.87 μM, suggesting that the affinity was reduced to 3.9-fold compared to canonical HP1α. We reasoned that Ub modification might disturb the intermolecular dimerization of HP1α CSDs probably because of the steric hindrance of Ub, which was elucidated for the first time by our study. It was envisaged that HP1α CSD might further reduce its affinity toward its CSD by being further attached with Ub chains.

Investigation of DNA binding ability of modified HP1α

To investigate the relationship between PTMs installed at the N-terminus, HR, or CSD and DNA-binding ability of HP1α, EMSAs were performed using 193-bp DNA. In this assay, HP1α without PTMs efficiently bound DNA, and its K_d value was 0.75 μM (Fig. 5B and C), which was consistent with the previous results.[66] **21a**, containing doubly phosphorylated Ser residues at its N-terminus, showed a slightly higher K_d value compared to normal HP1α (K_d: 1.32 μM), but **21b**, containing quadruple phosphorylation, significantly lowered the DNA-binding ability of HP1α (K_d: 4.67 μM). This result indicated that the number of phosphorylated Ser residues at the N-terminus of HP1α had an impact on its DNA-binding ability. We also evaluated the other PTMs on HR or CSD. **21c**, with double acetylation of Lys at HR, slightly lowered its DNA-binding ability (K_d: 1.79 μM), and these PTMs were found to be little influential. Surprisingly, **21d** and **21e** with Ser phosphorylation at HR had little influence on the affinity of HP1α toward DNA [K_d: 0.95 μM (**21d**), K_d: 0.82 μM (**21e**)], although basic patches on HR of HP1α were the main responsible sites for the interaction with DNA.[67] We found that

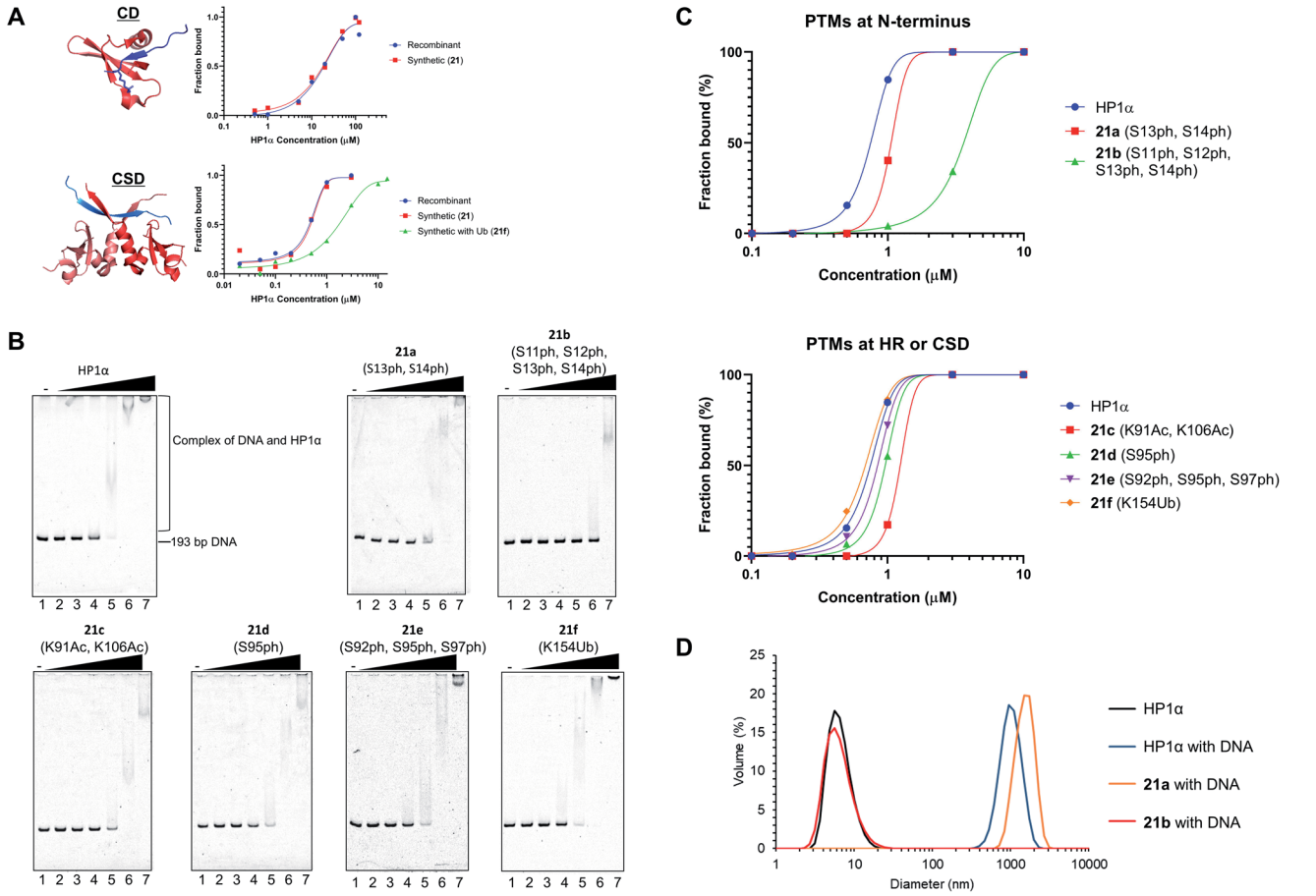

Fig. 5 Biochemical assays of chemically synthesized HP1αs. (A) Fluorescence anisotropy assay. Binding of the CD of recombinant HP1α or synthetic HP1α (**21**) with fluorescein-label H3 peptide bearing K9me3 (red: CD of HP1α, blue: N-terminal tail of histone H3 with K9me3, PDB: 3FDT) and binding of the CSD of recombinant HP1α, **21**, or **21f** with fluorescein-label Sgo1 peptide (red: CSD of HP1β, blue: Sgo1 peptide, PDB: 3Q6S). (B) EMSAs using chemically synthesized HP1α with PTMs. Representative gel images of the binding of HP1α toward DNA. Various concentrations of HP1α were incubated with 193-bp DNA. The complexes were analyzed by 8% native-PAGE and visualized with SYBR Gold. (C) Quantification of the EMSAs using HP1α with PTMs at **b** N-terminus, **c** HR or CSD. (D) DLS measurement of complexes composed of 193-bp DNA (50 nM) and modified HP1α (10 μM).

the binding affinity of **21f** with Ub at CSD was almost identical to that of normal HP1α (K_d: 0.71 μM).

Next, we analyzed the particle size of complexes composed of DNA and HP1α by DLS. HP1α without PTMs formed large particles with DNA, and its diameter was around 1000 nm (Fig. 5D). **21a** also formed large particles around 1000 nm diameter with DNA. However, **21b** dramatically inhibited the formation of complexes and we could not observe large particles, which would be caused by the lower DNA-binding ability of **21b**. Although HP1α possesses an acidic patch at its N-terminal (residues 15–19), HP1α has a higher binding ability toward DNA than other HP1 homologs. However, through the decoration of phosphorylations at S11–S14, HP1α significantly reduces its binding affinity by the extended acidic patch. Moreover, the number and location of phosphorylation were critical to control its DNA-binding ability, which would affect the behavior of HP1α in the nucleus. These significant discoveries in epigenetics were clarified by H1.2s and HP1αs with site-specific PTMs prepared through our new synthetic method using the organoruthenium catalyst.

Conclusions

We have developed a highly streamlined methodology for the chemical synthesis of various decorated proteins utilizing an air-tolerant organoruthenium catalyst. After the screening of organoruthenium complexes, we clarified that Ru complexes coordinated by Cp and *X*,*O*-bidentate ($X = N$ or P) ligand efficiently removed the alloc group in catalytic manners under NCL conditions, and that the TONs of **Ru-4** and **Ru-10** exceeded 70 even in the presence of 5000 equiv. of MPAA, which could not be achieved with other current metal complexes. The organoruthenium catalyst was applied for total chemical protein synthesis to produce linker histone H1.2 and HP1α with two and six different modification patterns and our technology afforded a large protein above 30 kDa (ubiquitinated HP1α). Especially for the synthesis of HP1α, by selecting appropriate metal complexes, we prevented the generation of aggregates during the synthetic procedure. Through the analysis of chromatosomes reconstituted by using three types of synthetic H1.2s *via* EMSAs, we discovered that R53Cit modification

contributed to the reduction of the binding affinity of H1.2 for nucleosomes. Furthermore, we revealed that four consecutive phosphorylations at S11–S14 of HP1α extended the acidic patch at its N-terminus, significantly reduced its DNA-binding ability, and disrupted the formation of complexes with DNA. With homogeneously modified proteins synthesized by using the Ru catalyst, the biological significance of the epigenetic marks on heterochromatin factors was elucidated. We believe that the streamlined chemical synthesis of proteins containing PTMs and other functional molecules with an organoruthenium catalyst would be a key for the elucidation of the mystery of biological phenomena and the creation of new therapeutic proteins.

Author contributions

N. K. performed all experiments, conceived and designed the project, and wrote the manuscript. T. K. performed reconstitution of chromatosomes. T. K., H. K., H. M. assisted in the writing of the manuscript and ESI.† A. O. and G. H. supervised the project and edited the manuscript.

Conflicts of interest

There are no conflicts to declare.

Acknowledgements

This work was supported by the Japan Society for the Promotion of Science (JSPS) KAKENHI 18H03931, 18H05504, and 19K22245 (A. O.), 18K05313, 19H05287, and 20H04704 and JST PRESTO JPMJPR19K6 (G. H.). N. K. was supported by a Research Fellow of the Japan Society for the Promotion of Science 19J13608. This work was also supported by JSPS KAKENHI JP18H05534, and the Platform Project for Supporting Drug Discovery and Life Science Research (BINDS) from Japan Agency for Medical Research and Development (AMED) under Grant Number JP20am0101076 and JST ERATO Grant Number JPMJER1901 (H. K.) and AMED under Grant Numbers 20he0622010h0001 (H. M.). We thank Dr Nozomu Suzuki (Nagoya University) to kindly allow us to measure CD spectra of recombinant and synthetic HP1αs. We also thank Dr Hiromi Takiguchi and Mr Tomohiro Kato for the measurement of Ru contents on synthetic proteins by using ICP-MS.

References

1 S. B. H. Kent, *Protein Sci.*, 2018, **28**, 313–328.
2 S. Bondalapati, M. Jbara and A. Brik, *Nat. Chem.*, 2016, **8**, 407–418.
3 J. W. Bode, *Acc. Chem. Res.*, 2017, **50**, 2104–2115.
4 A. C. Conibear, E. E. Watson, R. J. Payne and C. F. W. Becker, *Chem. Soc. Rev.*, 2018, **47**, 9046–9068.
5 V. Agouridas, O. El Mahdi, V. Diemer, M. Cargoët, J. M. Monbaliu and O. Melnyk, *Chem. Rev.*, 2019, **119**, 7328–7443.
6 K. Nakatsu, G. Hayashi and A. Okamoto, *Curr. Opin. Chem. Biol.*, 2020, **58**, 10–19.
7 R. B. Merrifield, *J. Am. Chem. Soc.*, 1963, **85**, 2149–2154.
8 P. E. Dawson, T. W. Muir, I. Clark-Lewis and S. B. H. Kent, *Science*, 1994, **266**, 776–779.
9 D. Bang, B. L. Pentelute and S. B. Kent, *Angew. Chem., Int. Ed.*, 2006, **45**, 3985–3988.
10 R. E. Thompson, X. Liu, N. Alonso-García, P. J. B. Pereira, K. A. Jolliffe and R. J. Payne, *J. Am. Chem. Soc.*, 2014, **136**, 8161–8164.
11 N. J. Mitchell, L. R. Malins, X. Liu, R. E. Thompson, B. Chan, L. Radom and R. J. Payne, *J. Am. Chem. Soc.*, 2015, **137**, 14011–14014.
12 C. Zuo, B. Zhang, B. Yan and J. S. Zheng, *Org. Biomol. Chem.*, 2019, **17**, 727–744.
13 E. Latocheski, G. M. Dal Forno, T. M. Ferreira, B. L. Oliveira, G. Bernardes and J. B. Domingos, *Chem. Soc. Rev.*, 2020, **49**, 7710–7729.
14 M. Jbara, E. Eid and A. Brik, *J. Am. Chem. Soc.*, 2020, **142**, 8203–8210.
15 J. M. Chalker, C. S. C. Wood and B. G. Davis, *J. Am. Chem. Soc.*, 2009, **131**, 16346–16347.
16 E. V. Vinogradova, C. Zhang, A. M. Spokoyny, B. L. Pentelute and S. L. Buchwald, *Nature*, 2015, **526**, 687–691.
17 S. D. Tilley and M. B. Francis, *J. Am. Chem. Soc.*, 2006, **128**, 1080–1081.
18 T. Schlatzer, J. Kriegesmann, H. Schröder, M. Trobe, C. Lembacher-Fadum, S. Santner, A. V. Kravchuk, C. F. W. Becker and R. Breinbauer, *J. Am. Chem. Soc.*, 2019, **141**, 14931–14937.
19 M. Jbara, S. K. Maity and A. Brik, *Angew. Chem., Int. Ed.*, 2017, **56**, 10644–10655.
20 M. Jbara, S. K. Maity, M. Seenaiah and A. Brik, *J. Am. Chem. Soc.*, 2016, **138**, 5069–5075.
21 S. K. Maity, M. Jbara, S. Laps and A. Brik, *Angew. Chem., Int. Ed.*, 2016, **55**, 8108–8112.
22 S. K. Maity, G. Mann, M. Jbara, S. Laps, G. Kamnesky and A. Brik, *Org. Lett.*, 2016, **18**, 3026–3029.
23 M. Jbara, S. Laps, S. K. Maity and A. Brik, *Chem.–Eur. J.*, 2016, **22**, 14851–14855.
24 M. Jbara, S. Laps, M. Morgan, G. Kamnesky, G. Mann, C. Wolberger and A. Brik, *Nat. Commun.*, 2018, **9**, 3154.
25 S. Laps, H. Sun, G. Kamnesky and A. Brik, *Angew. Chem., Int. Ed.*, 2019, **58**, 5729–5733.
26 M. Jbara, S. K. Maity and A. Brik, *Eur. J. Org. Chem.*, 2020, 3128–3132.
27 G. B. Vamisetti, G. Satish, P. Sulkshane, G. Mann, M. H. Glickman and A. Brik, *J. Am. Chem. Soc.*, 2020, **142**, 19558–19569.
28 S. Laps, G. Satish and A. Brik, *Chem. Soc. Rev.*, 2021, **50**, 2367–2387.
29 N. Kamo, G. Hayashi and A. Okamoto, *Angew. Chem., Int. Ed.*, 2018, **57**, 16533–16537.
30 L. S. Hegedus and R. W. McCabe, *Catalyst Poisoning*, Marcel Dekker, New York, 1984.
31 B. G. Poulson, K. Szczepski, J. I. Lachowicz, L. Jaremko, A.-H. Emwas and M. Jaremko, *RSC Adv.*, 2020, **10**, 215–227.

32 B. Koning, A. Meetsma and R. M. Kellogg, *J. Org. Chem.*, 1998, **63**, 5533–5540.
33 A. Kolpin, G. Jones, S. Jones, W. Zheng, J. Cookson, A. P. E. York, P. J. Collier and S. C. E. Tsang, *ACS Catal.*, 2017, **7**, 592–605.
34 Y. A. Lin, J. M. Chalker, N. Floyd, G. J. L. Bernardes and B. G. Davis, *J. Am. Chem. Soc.*, 2008, **130**, 9642–9643.
35 B. Sundararaju, M. Achard and C. Bruneau, *Chem. Soc. Rev.*, 2012, **41**, 4467–4483.
36 T. Kondo, Y. Morisaki, S. Uenoyama, K. Wada and T. Mitsudo, *J. Am. Chem. Soc.*, 1999, **121**, 8657–8658.
37 S. Tanaka, P. K. Pradhan, Y. Maegawa and M. Kitamura, *Chem. Commun.*, 2010, **46**, 3996–3998.
38 T. Völker, F. Dempwolff, P. L. Graumann and E. Meggers, *Angew. Chem., Int. Ed.*, 2014, **53**, 10536–10540.
39 M. D. Mbaye, B. Demerseman, J. L. Renaud, L. Toupet and C. Bruneau, *Angew. Chem., Int. Ed.*, 2003, **42**, 5066–5068.
40 B. Sundararaju, M. Achard, B. Demerseman, L. Toupet, G. V. M. Sharma and C. Bruneau, *Angew. Chem., Int. Ed.*, 2010, **49**, 2782–2785.
41 E. C. B. Johnson and S. B. H. Kent, *J. Am. Chem. Soc.*, 2006, **128**, 6640–6646.
42 K. Mashima, H. Kaneyoshi, S. Kaneko, A. Mikami, K. Tani and A. Nakamura, *Organometallics*, 1997, **16**, 1016–1025.
43 S. W. Harshman, N. L. Young, M. R. Parthun and M. A. Freitas, *Nucleic Acids Res.*, 2013, **41**, 9593–9609.
44 S. P. Hergeth and R. Schneider, *EMBO Rep.*, 2015, **16**, 1439–1453.
45 T. W. Flanagan and D. T. Brown, *Biochim. Biophys. Acta, Gene Regul. Mech.*, 2016, **1859**, 468–475.
46 A. Izzo and R. Schneider, *Biochim. Biophys. Acta, Gene Regul. Mech.*, 2016, **1859**, 486–495.
47 D. V. Fyodorov, B. R. Zhou, A. I. Skoultchi and Y. Bai, *Nat. Rev. Mol. Cell Biol.*, 2018, **19**, 192–206.
48 Recently, Hong *et al.* reported the chemical synthesis of linker histone H1.2 through sequential ligations on the solid phase. Z. Z. Hong, R. R. Yu, X. Zhang, A. M. Webb, N. L. Burge, M. G. Poirier and J. J. Ottesen, *bioRxiv*, 2019, DOI: 10.1101/661744.
49 Q. Wan and S. J. Danishefsky, *Angew. Chem., Int. Ed.*, 2007, **46**, 9248–9252.
50 M. A. Christophorou, G. Castelo-Branco, R. P. Halley-Stott, C. S. Oliveira, R. Loos, A. Radzisheuskaya, K. A. Mowen, P. Bertone, J. C. R. Silva, M. Zernicka-Goetz, M. L. Nielsen, J. B. Gurdon and T. Kouzarides, *Nature*, 2014, **507**, 104–108.
51 B. Sarg, W. Helliger, H. Talasz, B. Förg and H. H. Lindner, *J. Biol. Chem.*, 2006, **281**, 6573–6580.
52 K. Shintomi, M. Iwabuchi, H. Saeki, K. Ura, T. Kishimoto and K. Ohsumi, *Proc. Natl. Acad. Sci. U. S. A.*, 2005, **102**, 8210–8215.
53 J. Bednar, I. Garcia-Saez, R. Boopathi, A. R. Cutter, G. Papai, A. Reymer, S. H. Syed, I. N. Lone, O. Tonchev, C. Crucifix, H. Menoni, C. Papin, D. A. Skoufias, H. Kurumizaka, R. Lavery, A. Hamiche, J. J. Hayes, P. Schultz, D. Angelov, C. Petosa and S. Dimitrov, *Mol. Cell*, 2017, **66**, 384–397.
54 C. Maison and C. Almouzni, *Nat. Rev. Mol. Cell Biol.*, 2004, **5**, 296–305.
55 D. Canzio, A. Larson and G. J. Narlikar, *Trends Cell Biol.*, 2014, **24**, 377–386.
56 G. Nishibuchi and J. Nakayama, *J. Biochem.*, 2014, **156**, 11–20.
57 A. Kumar and H. Kono, *Biophys. Rev.*, 2020, **12**, 387–400.
58 J. S. Becker, D. Nicetto and K. S. Zaret, *Trends Genet.*, 2016, **32**, 29–41.
59 J. Kanga, J. Chaudharya, H. Donga, S. Kima, C. A. Brautigamb and H. Yu, *Mol. Biol. Cell*, 2011, **22**, 1181–1190.
60 S. Machida, Y. Takizawa, M. Ishimaru, Y. Sugita, S. Sekine, J. Nakayama, M. Wolf and H. Kurumizaka, *Mol. Cell*, 2018, **69**, 385–397.
61 G. LeRoy, J. T. Weston, B. M. Zee and N. L. Young, *Mol. Cell. Proteomics*, 2009, **8**, 2432–2442.
62 N. Kamo, G. Hayashi and A. Okamoto, *Chem. Commun.*, 2018, **54**, 4337–4340.
63 M. Jbara, E. Eid and A. Brik, *Org. Biomol. Chem.*, 2018, **16**, 4061–4064.
64 N. Kamo, G. Hayashi and A. Okamoto, *Org. Lett.*, 2019, **21**, 8378–8382.
65 T. Durek, V. Y. Torbeev and S. B. H. Kent, *Proc. Natl. Acad. Sci. U. S. A.*, 2007, **104**, 4846–4851.
66 K. Hiragami-Hamada, K. Shinmyozu, D. Hamada, Y. Tatsu, K. Uegaki, S. Fujiwara and J. Nakayama, *Mol. Cell. Biol.*, 2011, **31**, 1186–1200.
67 G. Nishibuchi, S. Machida, A. Osakabe, H. Murakoshi, K. Hiragami-Hamada, R. Nakagawa, W. Fischle, Y. Nishimura, H. Kurumizaka, H. Tagami and J. Nakayama, *Nucleic Acids Res.*, 2014, **42**, 12498–12511.
68 E. Minc, Y. Allory, H. J. Worman, J.-C. Courvalin and B. Buendia, *Chromosoma*, 1999, **108**, 220–234.
69 A. Chakraborty, K. V. Prasanth and S. G. Prasanth, *Nat. Commun.*, 2014, **5**, 3445.
70 G. Nishibuchi, S. Machida, R. Nakagawa, Y. Yoshimura, K. Hiragami-Hamada, Y. Abe, H. Kurumizaka, H. Tagami and J. Nakayama, *J. Biochem.*, 2019, **165**, 433–446.
71 S. Chen, C. Wang, L. Sun, D.-L. Wang, L. Chen, Z. Huang, Q. Yang, J. Gao, X.-B. Yang, J.-F. Chang, P. Chen, L. Lan, Z. Mao and F.-L. Sun, *Mol. Cell. Biol.*, 2015, **35**, 406–416.
72 S. Tang, L. J. Liang, Y. Y. Si, S. Gao, J. X. Wang, J. Liang, Z. Mei, J. S. Zheng and L. Liu, *Angew. Chem., Int. Ed.*, 2017, **56**, 13333–13337.